Phase transformations in Titanium: Anisotropic deformation of ω phase

2014 J. Phys.: Conf. Ser. 500 112042

(http://iopscience.iop.org/1742-6596/500/11/112042)

Journal of Physics: Conference Series **500** (2014) 112042 doi:10.1088/1742-6596/500/11/112042

Phase transformations in Titanium: Anisotropic deformation of ω phase

Hongxiang Zong[1,2], Dezhen Xue[1,2], Xiangdong Ding[1,2] and Turab Lookman[2]

[1] State Key Laboratory for Mechanical Behavior of Materials, Xi'an Jiaotong University, Xi'an 710049, China

[2] Theoretical Division, Los Alamos National Laboratory, Los Alamos, NM 87545, USA

Email: txl@lanl.gov

Abstract. We study the plastic deformation of the ω phase which is obtained when Titanium undergoes a phase transformation under pressure. We perform molecular dynamics simulations under uniaxial loading and find that the ω phase not only shows brittle fracture upon loading in the [0001] direction, but also exhibits "superplastic" deformation features along the $[10\bar{1}0]$ direction. The brittle fracture is analogous to that which occurs in metallic glass by means of shear banding whereas the ductility is mediated by the α (hcp) to ω (hexagonal) phase transformation. We further show that the elastic deformation of the ω phase is anisotropic; it can be non-uniform upon [0001] uniaxial compression. Our results provide insight into the mechanical behaviour of the ω phase and imply that the transformation mediated ductility can lead to improvement of the plasticity of ω-containing Titanium alloys.

1. Introduction

Phase transformation processes have a substantial impact on the inelastic and damage response of materials. Yet, our understanding of how different loading conditions affect volume fractions of transformed phases is very much in its infancy [1]. The group IV hexagonal close-packed (hcp) metals Zr, Ti and Hf, and their alloys have served as an excellent test-bed for studying aspects of deformation and phase transformation behaviour under different conditions. For the hexagonal closed packed α (hcp) to ω (hexagonal) phase transformation, progress over the last three decades from recovery experiments and analysis of wave profiles [1-3] has largely focused on capturing the behavior of the equation of state, orientation relationships in microstructures, understanding the influence of impurities such as oxygen, and characterizing the deformation. Noteworthy is that the high pressure ω phase is highly metastable and retained on release under ambient conditions.

Titanium (Ti) and its alloys are of considerable technological importance in the aerospace, nuclear, and biomedical industries due to their high strength, light weight, corrosion resistance, and nuclear absorption cross sections [4-6]. However, the ω phase is quite brittle and can always be found either in β-

stabilized Titanium alloys or in pure Titanium under rapid cooling, aging or shock conditions [7-9]. More recently, high pressure torsion (HPT) studies have demonstrated how relatively large volume fractions of submicron crystalline retained ω phases can be obtained in Ti (~ 90%) and Zr (almost 100%) at room temperature [10-12]. It has been shown that the presence of ω phase not only has profound effects on mechanical properties, such as the increase in microhardness with consequent loss of ductility [13, 14], but also on transport and superconductive properties [15, 16]. Thus, an understanding of deformation and phase transformation behavior in the ω phase is of the utmost interest, given the practical importance of Titanium based alloys.

The brittleness of ω-containing alloys is usually associated with either crack initiation around an inherently brittle ω precipitate or the obstruction of slip in the bcc-β phase [7, 13]. The mechanical behavior of the ω phase, however, remains unclear [17]. Crystallographically, the ω phase has a layered hexagonal non-closed-packed structure: the first layer A consists of atoms at Wyckoff position (000) and the next layer B has atoms at the Wyckoff positions $\left(\frac{2}{3}\frac{1}{3}\frac{1}{2}\right)$ and $\left(\frac{1}{3}\frac{2}{3}\frac{1}{2}\right)$. Although the chemical bonding in the A layer is metallic, the atomic interactions within the B layer consist of covalent bonds based on sp2 hybridized orbitals. The bonds between the A and B layers are also covalent [18]. In addition, as these atomic layers are rather corrugated, the atomic planes cannot slip/slide past each other very easily [19]. As a result, one may expect the ω phase not to be plastically deformable. However, experimental results are far from being clear on this issue. A number of experiments show that the ω phase is brittle, which is consistent with theoretical predications. The fracture mechanism of some Titanium based alloys, e.g., Ti-10%Mo, is considered to involve "shear banding" [13]. However, experiments also show that the ω phase can be transformed to the hexagonally closed packed (hcp) α phase under compression, which indicates that the ω phase may show some pseudo plastic deformation mediated by the ω to α phase transformation [20, 21].

In this letter, we study the deformation behavior of ω phase in pure Titanium to explore these questions using molecular dynamic (MD) simulations. We find that anisotropy in the deformation of the ω phase plays a crucial role that can help to explain the range of behavior seen in experiments. The crystal exhibits elastic deformation, followed by a strength drop immediately after yielding, i.e., brittle fracture, when deformed in tension and compression along the $[10\bar{1}0]$ direction. However, under compression loading along the $[10\bar{1}0]$ direction, the ω phase undergoes a martensitic phase transformation to the α phase. The phase transformation, together with the reorientation of α phase twins and dislocations in α phase, leads to "superplastic" deformation behavior of more than 30% strain. This can be utilized, in principle, to improve the ductility of titanium alloys even in the presence of the ω phase.

2. Computational methods

Our simulations for a perfect ω Titanium crystal under uniaxial loading have the x axis of the simulation box oriented along the [0001] or $[10\bar{1}0]$ crystallographic directions with periodic boundary conditions in all directions. Typical samples contained 57600 atoms with dimensions $L_{[10\bar{1}0]}$= 7.4 nm, $L_{[0001]}$= 8.0 nm and $L_{[1\bar{2}10]}$=17.1 nm or 216000 atoms with dimensions $L_{[0001]}$ = 18.4 nm, $L_{[10\bar{1}0]}$ =17.6 nm and $L_{[1\bar{2}10]}$=17.1 nm. The interatomic interactions in Titanium were described by a spline-based modified embedded atom method (MEAM) potential, which was specifically developed to simulate the ω structure [22]. An isothermal-isobaric ensemble was adopted, in which Nosé-Hoover thermostat and Parrinello–Rahman barostat are used to control the temperature and pressure of the system. After constructing the initial structures, the ensembles were then minimized to their lowest potential energy state by a conjugate gradient method, and then followed by 100 ps aging at 100 K and 1 atm. The aged sample was then deformed by applying tensile or compressive uniaxial strain at a rate of 10^9 s^{-1}. The MD calculations were carried out using the LAMMPS code [23] with the atomic configurations visualized using the local crystal structure technique of Ackland [24].

3. Results and discussion

In the following we present results of several tensile and compression simulations. Specifically, we focus on two deformation mechanisms: brittle fracture and phase transformation mediated ductile plastic deformation.

3.1 Tension deformation behavior along [0001] direction.

We first measured the deformation behavior of the ω phase in uniaxial tension along the [0001] direction. Figure 1a shows the corresponding stress-strain curves of the ω phase when loaded at 100 K. After an elastic deformation up to the yield point at 21.4 GPa, the stress drops to zero immediately. This is typical brittle fracture behavior. The atomic configurations during the course

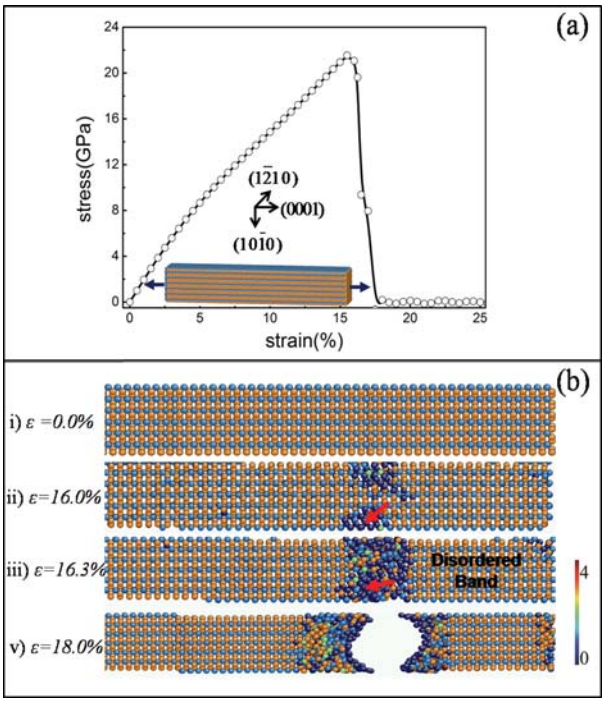

Figure 1. The mechanical response of ω-Ti under [0001] uniaxial tension. (a) Stress-strain curve at 100 K (b) Atomic configurations associated with the fracture process as a function of strain starting from an undeformed ω lattice (stacked layers). The blue and orange signify nucleation (arrow) and progression of local structure (shear bands).

of the fracture process (shown in figure 1b) allow us to identify the nature of the brittle fracture in this ω pillar under [0001] tension. We find that after yielding, disordered bands first nucleate from the interior of the sample (figure 1b(ii)) and then expand dramatically, undergoing a stress-driven amorphization process (figure 1b(iii)). Macrocracks are finally generated that lead to the fracture of the sample. The formation of disordered bands after yielding is often observed if covalent bonds are dominant. The external stress after the yield stress is large enough to break these covalent bonds, and leads to regions with comminuted material locally, acting as nucleation sites for an order-disorder type transformation. Such deformation behavior is also observed in SiC in which local ‘‘shear transformation zones’’ (STZs) undergo shear localization due to particle break-up (comminution) and rearrangement of the comminuted zones [25, 26].

3.2 Compression deformation behavior along [0001] direction

For brittle materials such as SiC, ceramics and metallic glasses, the asymmetry of the mechanical behavior under tension and compression has been widely observed. However, in this regard little is known about the ω phase and we therefore investigate its mechanical response under [0001] uniaxial compression, the results are shown in figure 2. Similar to the deformation behavior observed under [0001] uniaxial tension (figure 1), we find that under uniaxial [0001] compression ω also shows brittle fracture behavior. The

stress-strain behavior falls off sharply after the yield point (figure 2a), and during the fracture process,the disordered bands are

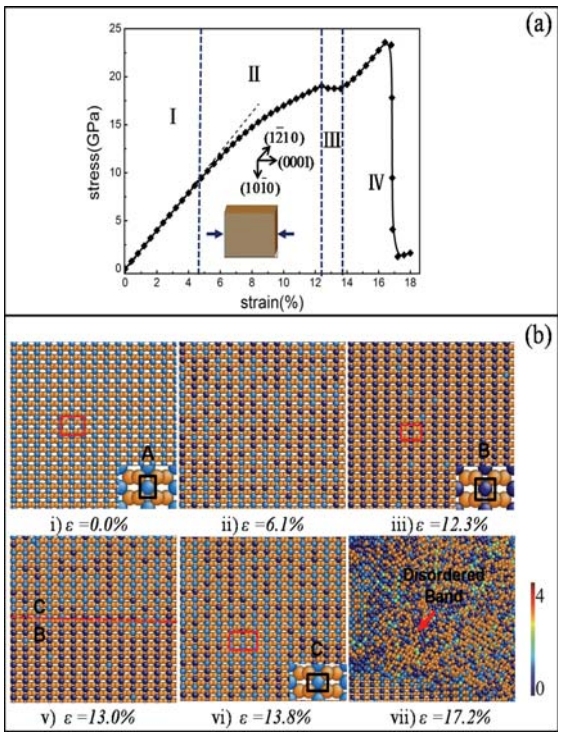

Figure 2. The mechanical response of ω-Ti under [0001] uniaxial compression (a) Stress-strain curve at 100 K. (b) Atomic configurations corresponding to the stress-strain curve in (a) showing the structural changes (A to B to C) as a function of strain. The final configuration shows shear banding (red arrow) mediated fracture.

seen to extend into the whole sample (figure 2b(vii)). The elastic deformation under [0001] uniaxial compression however differs from that under [0001] uniaxial tension. It includes four regimes: a linear deformation regime (I), a nonlinear regime (II), a regime with a stress plateau (III) and another linear deformation regime (IV). These features arise due to the nonuniform elastic deformation of ω-Ti that is quite unlike the uniform elastic deformation seen in most metals. Following the uniform elastic regime (I) for perfect ω-Ti, in regime II the original ω structure (cell-A in figure 2b(i)) transforms to a metastable structure (cell-B in figure 2b(iii)) and this transformation is mediated by random nucleation of cell-B from cell-A, the phase with cell-B grows at the expense of cell-A which disappears (figure 2b(ii)). Further compression leads to the transformation of cell-B to another metastable structure (cell-C in figure 2b(vi)) in region III. The atomic configurations are shown in figure 2b(iii to vi). The transformation from metastable B to C is mediated by the movement of an interface between these metastable structures (figure 2b(v)). Such interface movement is usually energetically preferred compared to random nucleation and growth in region II, thus this transformation can occur in a small strain region, and leads to a short plateau in region III. Region IV is again the uniform elastic deformation of the metastable structure C.

From the above, we learn that the elastic deformation of ω-Ti phase is mediated by a sequence of structure transformations, i.e., from the original structure A to a metastable structure B and finally to metastable structure C. To understand the underlying reasons, we calculated the potential energy of the ω-Ti primitive cell under c-axis compression. The results show that there are two energy minima in the behavior of the potential energy as a function of the strain along the c-axis (figure 3), consistent with the two metastable structures observed above. Further

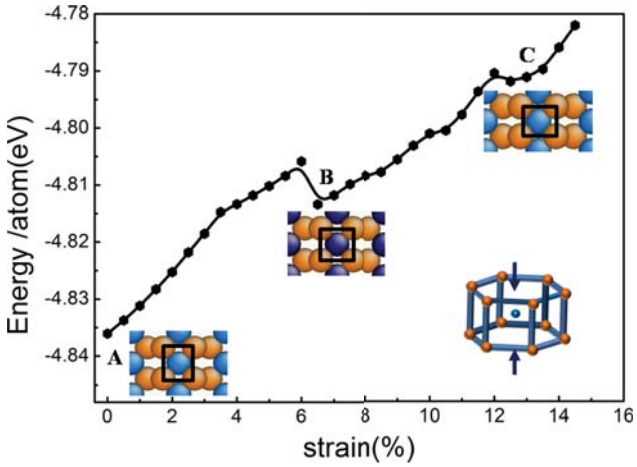

Figure 3. The average potential energy per atom of the ω structure as a function of strain under c-axis compression. The initial, perfect ω structure (A) transforms to metastable structures (B) and (C) with orthorhombic symmetry.

calculation shows that the metastable structure B has orthorhombic symmetry, Cmmm, with lattice parameters a=4.763 A and c/a=0.517, whereas the metastable structure C has orthorhombic symmetry Pmm2, with a=9.521 A, b=8.256 A and c= 4.874 A.

3.3 Compression deformation behaviour along $[10\bar{1}0]$ *direction*

We further studied the mechanical behavior of ω phase under $[10\bar{1}0]$ uniaxial compression and find a plastic deformation mechanism not seen previously. Referring to the stress-strain curve shown in figure 4a, we find that after the initial elastic deformation (I) the ω to α phase transformation occurs (II). Further loading leads to rotation of the α variants and the emission of dislocations (III) which provide plastic deformation of more than 30%. The atomic evolution under $[10\bar{1}0]$ uniaxial compression is shown in figure 4b. The yield point after the elastic deformation (regime I) occurs at about 8 GPa, which is much lower than that under [0001] uniaxial loading (about 24 GPa). The atomic configurations at the yield point show that an intermediate phase (an orthorhombic phase, blue regions in figure 4b(i)), rather than the disordered bands (which occurred under [0001] uniaxial loading), nucleates from the ω-Ti phase. That is the reason for the relatively low yielding strength under $[10\bar{1}0]$ compression. Further loading after yield leads to the ω to α phase transformation (region II of figure 4a). The intermediate phase first grows into the ω matrix, and then the α phase nucleates in this intermediate phase and grows. The whole ω matrix finally transforms to the α phase (figure 4b(iii)). Thus, this transformation is characterized by a sudden drop in the stress-strain curve, and is mediated though the intermediate, orthorhombic phase, in contrast to a direct transformation to α. This evolution is consistent with a previous experimental observation that a γ phase (a distorted hcp or orthorhombic phase) [27] mediates the transformation.

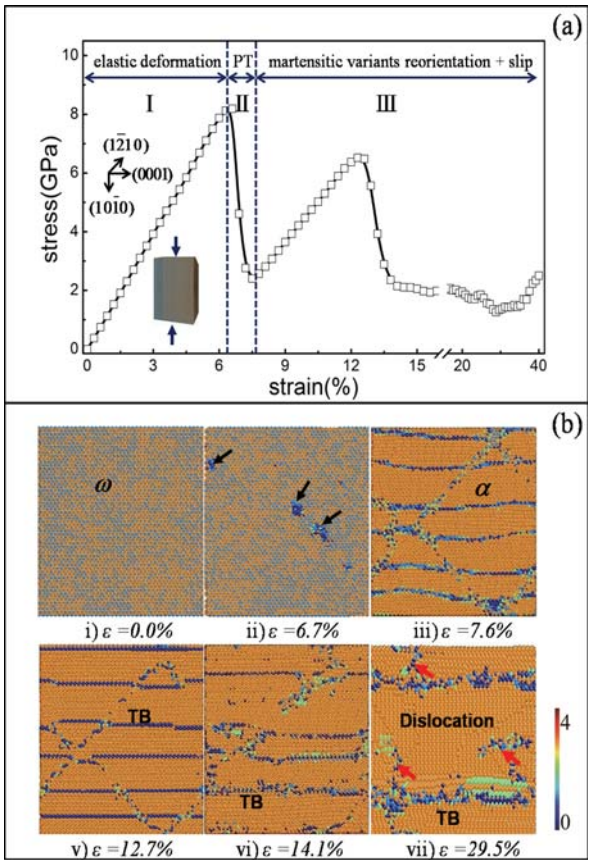

Figure 4. The mechanical response of ω under [10$\bar{1}$0] uniaxial compression. (a) Stress-strain curve with elastic deformation (I) followed by transformation (II) and plastic deformation (III)., (b) Snapshots of the microstructure evolution during the deformation process. The black arrows indicate nucleation of α which transforms into variants followed by plastic deformation. The red arrows indicate dislocations.

We note that a twinned structure is formed in the α phase towards the latter part of the transformation. The twin-boundary plane (the {10$\bar{1}$1} twin boundary, marked as TB in figure 4b(iii)) is perpendicular to the loading direction. Increasing the applied strain (region III of figure 4a) in the transformed α first causes the elastic deformation of α , and then some of the newly formed α variants rotate by 60° to a preferred orientation (figure 4b(vi)), resulting in stress release. This phenomenon is widely observed in ferroelastic materials as a "de-twinning" process [28]. If we further load the sample, a few of the slip systems of α Ti are initiated due to higher local stress, and the emission of dislocations in the α phase provides additional plastic deformation (figure 4b(vii)). It's important to recognize that the total strain in regime III is more than 30%, and this is a substantial contribution to the "superplastic" deformation behavior.

3.4 Mechanism of anisotropic deformation

As it is impossible to completely eliminate the brittle ω phase in Titanium alloys, our results imply that one can increase the ductility of ω-containing Titanium alloys by distributing ω phase precipitates with preferred orientations. If the ω phase precipitates can form strong texture along the [10$\bar{1}$0] orientation (e.g., through preferred orientation growth or shock), a simple uniaxial compression along the [10$\bar{1}$0] direction will improve toughness and ductility in ω-containing Titanium alloys.

The key point in understanding why ω transforms to α under [10$\bar{1}$0] uniaxial compression, instead of undergoing brittle fracture as occurs along [0001] , is the anisotropic resolved shear stress that acts on the ω to α shear system [29]. The anisotropy of the resolved shear stress can be characterized by an orientation factor (Schmid factor) [30, 31], which is the ratio between the resolved shear stress on the

phase transformation shear system and the uniaxial stress, i.e., $f_{OR} = {}^{\tau}/_{\sigma} = \cos\phi\cos\lambda$, where $\phi$is the angle between the normal vector of the phase transformation plane and the loading direction, and $\lambda$the angle between the shear direction of the phase transformation plane and the loading direction. The transformation system with the highest orientation factor is the easiest one to be activated. Under [0001] uniaxial loading, the orientation factor for the transformation shear systems is 0.12. The shear system we use is the $(0\bar{1}11)[01\bar{1}1]$ transformation system which corresponds to the TAO-1 transformation pathway that was recently proposed for $\alpha \rightarrow \omega$ [32]. Thus, the critical stress to induce phase transformation is calculated to be roughly 60 GPa, which is more than twice the brittle fracture yield point of 21.4 GPa. Hence, only STZ mediated brittle fracture occurs under [0001] uniaxial loading. However, under $[10\bar{1}0]$ loading the orientation factor for the transformation shear systems is 0.89. This means that only 8 GPa is needed to induce the ω to α phase transformation upon $[10\bar{1}0]$ uniaxial compression.

4. Conclusion

In summary, we have shown that the ω phase undergoes anisotropic deformation behaviour and we have presented a mechanism which in principle can improve the ductility of Titanium alloys in the presence of this phase. In particular, we propose a phase transformation mediated mechanism for the plastic deformation mechanism associated with the ω phase in the $[10\bar{1}0]$ direction. This is in contrast to the brittle fracture that occurs along the [0001] direction. We believe that the mechanism is not limited to Titanium alloys but should also apply to other group IV transition elements such as Zr and Hf.

Acknowledgments

This work was supported by NSFC (51171140, 51231008), the 973 Program of China (2010CB631003, 2012CB619402) and 111 project (B06025), as well as US DOE at LANL (DE-AC52-06NA25396).

Reference

[1] Cerreta E, Gray III G T, Hixson R S, Rigg P A and Brown D W 2005 *Acta Mater*. **53** 1751
[2] Song G and Gray III G T 1995 *Philos*. *Mag*. A **71** 275
[3] Cerreta E, et al. 2007 *AIP Conf*. *Proc*. **955** 635
[4] Leyens C and Peters M 2006 Titanium and Titanium Alloys (New York: John Wiley & Sons)
[5] Geetha M, Singh A K, Asokamani R and Gogia A K 2009 *Prog*. *Mater*. *Sci*. **54** 397
[6] Schutz R W and Watkins H B 1998 *Mater*. *Sci*. *Eng*. A **243** 305
[7] Hickman B S 1969 *J*. *Mater*. *Sci*. **4** 554
[8] Jamieson J C 1963 *Science* **140** 72
[9] Perez-Prado M T, Gimazov A A, Ruano O A, Kassner M E and Zhilyaev A P 2008 *Scripta Mater*. **58** 219
[10] Errandonea D and Meng Y, Somayazulu M and Hausermann D 2005 *Physica* B **355** 116
[11] Todaka Y, Sasaki J, Moto T and Umemoto M 2008 *Scripta Mater*. **59** 615
[12] Edalatia, Horitaa Z, Yagib S and Matsubarab E 2009 *Mat*. *Sci*. *& Eng*. A **523** 277
[13] Williams J, Hickman B and Marcus H 1971 *Metall*. *Mater*. *Trans*. B **2** 1913
[14] Zhang S Q, Li S J, Jia M T, Prima F, Chen L J, Hao Y L and Yang R 2011 *Acta Mater*. **59** 4690
[15] Myron H W, Freeman A J and Moss S C 1975 *Solid State Commun*. **17** 1467
[16] Narasimhan S L, Taggart R and Polonis D H 1976 *J*. *Mater*. *Sci*. **11** 134
[17] Sikka S K, Vohra Y K and Chidambaram R 1982 *Prog*. *Mater*. *Sci*. **27** 245
[18] Doherty J E and Gibbons D F 1971 *Acta Metall*. **19** 275
[19] Zhao Y and Zhang J 2007 *Appl*. *Phys*. *Lett*. **91** 1907
[20] Bychkov L Y N, Yu F and Mal'tsev V A 1973 *Fiz*. *Metal*. *Metalloved* **36** 413
[21] Bychkov L Y N, Yu F and Mal'tsev V A 1974 *Fiz*. *Metal*. *Metalloved* **38** 1294

[22] Hennig R G, Lenosky T J, Trinkle D R, Rudin S P and Wilkins J W 2008 *Phys. Rev.* B **78** 054121
[23] Plimpton S 1995 *J. Comput. Phys.* **117** 1
[24] Ackland G J and Jones A P 2006 *Phys. Rev.* B **73** 054104
[25] Shih C J, Meyers M A and Nesterenko V F 1998 *Acta Mater.* **46** 4037
[26] Romano A, Li J and Yip S 2006 *J. Nucl. Mater.* **352** 7
[27] Vohra Y K and Spencer P T 2001 *Phys. Rev. Lett.* **86** 3068
[28] Orlovskaya N, Browning N and Nicholls A 2003 *Acta Mater.* **51** 5063
[29] Jaworski A and Ankem S 2005 *Rev. Adv. Mater. Sci.* **10** 11
[30] Fromm B S, Adams B L, Ahmadi S and Knezevic M 2009 *Acta Mater.* **57** 2339
[31] Koike J and Ohyama R 2005 *Acta Mater.* **53** 1963
[32] Trinkle D R, Hennig R G, Srinivasan S G, Hatch D M, Jones M D, Stokes H T, Albers R C and Wilkins J W 2003 *Phys. Rev. Lett.* **91** 025701